Determination of the Fermi Velocity by the High-Field Tilt Effect*

HAROLD N. SPECTOR
Institute for the Study of Metals, University of Chicago, Chicago, Illinois
(Received July 14, 1960)

The attenuation of a sound wave in a semimetal in the presence of a magnetic field is examined when the magnetic field is tilted from the direction perpendicular to the direction of propagation of the sound wave. It is found that in the limit of high magnetic fields ($\omega_c\tau \geq 10ql$) the behavior of the attenuation with the angle of tilt gives a point-by-point determination of the velocity on the Fermi surface. A detailed treatment of a two-spherical-band model is given and the case of a general Fermi surface is examined qualitatively.

I. INTRODUCTION

RECENT experiments[1] on the attenuation of ultrasonic waves in semimetals at liquid helium temperatures have revealed a strong dependence of the attenuation on the relative orientation of the magnetic field and the direction of propagation. The attenuation has been observed to increase by a factor as large as four when the field is tilted by a small angle ν away from a direction perpendicular to the direction of propagation. The following qualitative explanation of this phenomenon has been given by Reneker.[1] He relates the increase in attenuation to the advance of planes of constant phase past the electrons as they spiral along the magnetic field. As the magnetic field is tilted by an angle ν, the average drift velocity of a carrier along the magnetic field develops a component $V_H \sin\nu$ along the direction of propagation. The phase velocity relative to the carrier is reduced from V_S to $V_S - V_H \sin\nu$, where V_S is the velocity of the sound wave. When the tilt reaches a critical angle ν_c, where $\sin\nu_c = V_S/(V_H)_{\max}$, the phase velocity relative to the carrier becomes zero and the fastest carrier experiences a steady acceleration. For still larger angles of tilt, slower carriers experience a steady acceleration. Thus, at the critical angle ν_c, there should be an abrupt increase in attenuation. By determining the critical angle we can determine accurately the ratio V_S/V_F since the maximum velocity of drift $(V_H)_{\max}$ is the Fermi velocity V_F. As the velocity of sound is readily measured for all directions of propagation, V_F can be determined point by point on the Fermi surface.

In Sec. II we give a quantitative treatment of the high-field tilt effect based on Harrison's theory of ultrasonic attenuation in semimetals.[2] We are interested in relating the behavior of the attenuation to the critical angle ν_c and examining the dependence of attenuation on $\omega\tau$ and the magnetic field. In Sec. III we give a discussion of the results of the calculation in Sec. II and the applicability of the results to an actual experiment. In Sec. IV we examine the case of a general Fermi surface.

* This research was supported in part by the National Science Foundation.
[1] D. H. Reneker, Phys. Rev. **115**, 303 (1959).
[2] M. J. Harrison, Phys. Rev. **119**, 1260 (1960).

II. DERIVATION OF THE ATTENUATION

Cohen, Harrison, and Harrison[3] have derived a general expression for the conductivity tensor in the coordinate system of the magnetic field using a free-electron model. We shall use this expression for the conductivity tensor to derive the components of the tensor in the high-field case, i.e., $\omega_c\tau \geq 10ql$. We take the direction of the magnetic field as the z axis of our coordinate system and the y axis perpendicular to the plane containing both the magnetic field and the direction of propagation. The x axis is defined as the remaining direction of a right-handed orthogonal triad. Then we obtain the following elements of the conductivity tensor in the high-field limit:

$$\sigma_{xx}=\frac{(1-i\omega\tau)\sigma_0}{(\omega_c\tau)^2} \qquad \sigma_{xy}=-\sigma_{yx}=\frac{-\sigma_0}{\omega_c\tau},$$

$$\sigma_{yy}=\frac{(1-i\omega\tau)\sigma_0}{(\omega_c\tau)^2}+\frac{3}{8}\frac{ql\cos^2\nu\sigma_0}{(\omega_c\tau)^2}\Bigg[\left(1+\frac{2(1-i\omega\tau)^2}{(ql\sin\nu)^2}+\frac{(1-i\omega\tau)^4}{(ql\sin\nu)^4}\right)[G(\omega\tau,\nu)+iH(\omega\tau,\nu)]-\frac{10}{3}\frac{(1-i\omega\tau)}{ql\sin^2\nu}-\frac{2(1-i\omega\tau)^3}{(ql)^3\sin^4\nu}\Bigg], \quad (2.1)$$

$$\sigma_{zz}=\frac{3(1-i\omega\tau)\sigma_0}{(ql\sin\nu)^2}-\frac{3}{2}\frac{(1-i\omega\tau)^2\sigma_0}{(ql)^3\sin^2\nu}\times[G(\omega\tau,\nu)+iH(\omega\tau,\nu)],$$

$$\sigma_{xz}=\sigma_{zx}=0, \quad \sigma_{yz}=\sigma_{zy}=0,$$

$$G(\omega\tau,\nu)=\frac{\arctan(\omega\tau+ql\sin\nu)-\arctan(\omega\tau-ql\sin\nu)}{\sin\nu},$$

$$H(\omega\tau,\nu)=\ln\left[\frac{1+(\omega\tau+ql\sin\nu)^2}{1+(\omega\tau-ql\sin\nu)^2}\right]\Big/2\sin\nu,$$

where $\pi/2-\nu$ is the angle between the magnetic field and the direction of propagation. The other quantities

[3] M. H. Cohen, M. J. Harrison, and W. A. Harrison, Phys. Rev. **117**, 937 (1960).

appearing in the expression are the dc conductivity σ_0, the cyclotron frequency ω_c, the sound wave number q and frequency ω, and the relaxation time τ.

We now transform the conductivity tensor to the coordinate system where the direction of propagation of the sound wave is along the 1 direction and the 2 direction corresponds to the y direction of our first coordinate system.

$$\sigma_{11}=\frac{(1-i\omega\tau)\cos^2\nu\sigma_0}{(\omega_c\tau)^2}-\frac{3}{2}\frac{(1-i\omega\tau)^2\sigma_0(G+iH)}{(ql)^3}+\frac{3(1-i\omega\tau)\sigma_0}{(ql)^2},$$

$$\sigma_{22}=\frac{(1-i\omega\tau)\sigma_0}{(\omega_c\tau)^2}+\frac{3}{8}\frac{ql\cos^2\nu\sigma_0}{(\omega_c\tau)^2}\times\left[\left(1+\frac{2(1-i\omega\tau)^2}{(ql\sin\nu)^2}+\frac{(1-i\omega\tau)^4}{(ql\sin\nu)^4}\right)(G+iH)-\frac{10}{3}\frac{(1-i\omega\tau)}{ql\sin^2\nu}-\frac{2(1-(\omega\tau)^3}{(ql)^3\sin^4\nu}\right],\quad(2.2)$$

$$\sigma_{33}=\frac{(1-i\omega\tau)\sin^2\nu\sigma_0}{(\omega_c\tau)^4}-\frac{3}{2}\frac{(1-i\omega\tau)^2\cot^2\nu\sigma_0(G+iH)}{(ql)^3}+\frac{3(1-i\omega\tau)\cot^2\nu\sigma_0}{(\omega_c\tau)},$$

$$\sigma_{12}=-\sigma_{21}=\frac{-\sigma_0}{\omega_c\tau}\cos\nu\quad\sigma_{23}=-\sigma_{32}=\frac{-\sigma_0}{\omega_c\tau}\sin\nu,$$

$$\sigma_{13}=\sigma_{31}=\frac{3(1-i\omega\tau)\cot\nu\sigma_0}{(ql)^2}-\frac{3}{2}\frac{(1-i\omega\tau)^2\cot\nu\sigma_0}{(ql)^3}\times(G+iH)-\frac{1}{2}\frac{(1-i\omega\tau)\sin2\nu\sigma_0}{(\omega_c\tau)^2}.$$

Harrison,[2] using a two-spherical-band model with the effective masses, relaxation times, and deformation potentials the same for both bands, derives the following expression for the attenuation per unit length in the direction of propagation for a semimetal:

$$\alpha=(2Nm/\rho V_S\tau)S_{11}.\quad(2.3)$$

In Eq. (2.3), ρ is the mass density of the semimetal, m the free electron mass, N the number of carriers, and

$$S_{11}=1-\frac{m}{m^*}\mathrm{Re}\left\{\left(1+\frac{iV_D\tau q^2}{m\omega}\right)^2\sigma_{11}'\right\},\quad(2.4)$$

where m^* is the effective mass of the carriers and V_D is the deformation potential. From CHH[3] we have

$$\boldsymbol{\sigma}'=[\mathbf{I}-\mathbf{R}]^{-1}\frac{\boldsymbol{\sigma}}{\sigma_0},\quad(2.5)$$

where $\boldsymbol{\sigma}$ is the conductivity tensor and

$$R_{ij}=R_i\delta_{ij},\quad R_{i1}=\frac{-i\omega\tau V_F^2\sigma_{i1}}{3\sigma_0(1-i\omega\tau)V_S^2}.\quad(2.6)$$

For our case

$$\sigma_{11}'=\frac{\omega\tau(1-i\omega\tau)}{(ql)^2}\times\frac{[(ql/\omega_c\tau)^2\cos^2\nu+3(N-iM)]}{\omega\tau+M+i[\frac{1}{3}(ql/\omega_c\tau)^2\cos^2\nu+N]}.\quad(2.7a)$$

$$M=\frac{H-\omega\tau G}{2ql},\quad N=1-\frac{(G+\omega\tau H)}{2ql}.\quad(2.7b)$$

In the case of bismuth[2] it was estimated that $V_D/mV_F^2\sim20$ so that in S_{11} only the terms in $(V_D/mV_F^2)^2$ need be kept. Therefore we have for S_{11}

$$(S_{11}-1)\Big/\frac{m}{m^*}\left(\frac{V_D}{mV_F^2}\right)^2=\frac{(ql)^2\{3M(\omega\tau+M)+[\frac{1}{3}(ql/\omega_c\tau)^2\cos^2\nu+3-N][(ql/\omega_c\tau)^2\cos^2\nu+3N]\}}{\{(\omega\tau+M)^2+[\frac{1}{3}(ql/\omega_c\tau)^2\cos^2\nu+N]^2\}}.\quad(2.8)$$

III. NUMERICAL RESULTS AND DISCUSSION

The function $(S_{11}-1)/(m/m^*)(V_D/mV_F^2)^2$ has been plotted vs the angle of tilt ν for various values of $\omega\tau$ in Fig. 1. When the angle of tilt increases from zero, the function initially increases slowly. As we approach ν_c, the function begins a rapid increase, the rate of increase depending upon whether $\omega\tau>1$ or not. For $\omega\tau>1$ the increase is very sharp while for $\omega\tau<1$ the increase is more gradual. When $\omega\tau>1$, the function has an inflection point at ν_c. The inflection point becomes less noticeable and is shifted in position to angles $>\nu_c$ when $\omega\tau<1$. Beyond the critical angle, the function reaches a peak value. The height of the peak is roughly proportional to $\omega\tau$ for the range of $\omega\tau$ considered. The position of the peak and the position of the inflection point have been plotted vs $\omega\tau$ in Fig. 2. As the value of $\omega\tau$ decreases, the position of both the peak and the inflection point of the function are shifted over to larger angles of tilts. After reaching its peak value the function falls off roughly as $1/\sin\nu$ as ν increases to $\pi/2$.

These results are valid in the high-field case, i.e., when $\omega_c\tau\geq10ql$. As long as we remain in the high-field region, the position of the inflection point and the peak remain unchanged when $\omega\tau\geq1$. The effect of the magnetic field in this case is to change the initial

height of the function at $\nu=0$ and not to change the general shape of the function.

When $\omega\tau>1$, the position of the inflection point is exactly at ν_c and therefore gives us an accurate determination of V_F. Even for $\omega\tau=1$, the shift of the position of the inflection point from ν_c is only 12.5%. When $\omega\tau<1$, the curves in Fig. 1 cannot be used to determine V_S/V_F directly since the inflection point no longer falls close to ν_c.

To determine ν_c for $\omega\tau<1$, we must use Fig. 3 where the ratio of ν_c to the position of the inflection point ν_i is plotted vs the ratio of the position of the peak ν_p to the position of the inflection point. Since we can measure the positions of the peak and the inflection point, we can read off the value of ν_c directly from Fig. 3.

The curves in Fig. 1 and Fig. 2 can be used for any

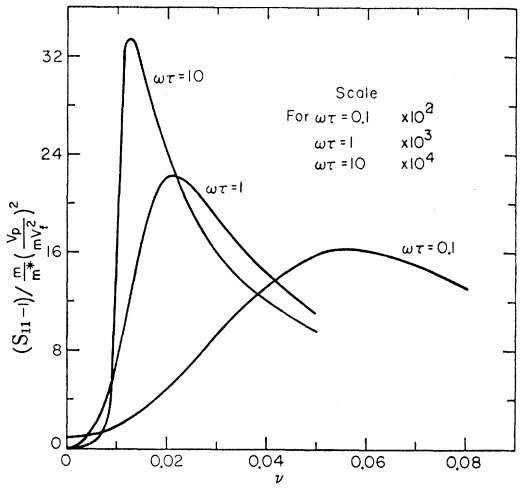

FIG. 1. The normalized attenuation

$$(S_{11}-1)/[(m/m^*)(V_D/mV_F^2)^2]$$

as a function of the angle of tilt ν for values of $\omega\tau=0.1$, 1, and 10 when the condition $V_0/mV_F^2\gg1$ is satisfied.

substances in which the model used is correct, since the function $(S_{11}-1)/[(m/m^*)(V_D/mV_F^2)^2]$ is a universal function of $(V_F/V_S)\sin\nu$ and $\omega\tau$. Using values of m/m^* and V_D/mV_F^2 estimated for bismuth,[2] we see from the curves in Fig. 1, that the function plotted is $\alpha\rho V_S\tau/[2Nm(m/m^*)(V_D/mV_F^2)^2]$, i.e., it is a normalized attenuation. Therefore, the behavior of the attenuation with angle of tilt is the same as the function plotted in Fig. 1.

The predicted sharp rise in the attenuation near the critical angle and the peak lying beyond ν_c are very similar to those features observed and interpreted by Reneker.[1] The peak arises from the appearance in the σ_{zz} component of the conductivity tensor of a resonance denominator. Before performing the integrations leading to Eq. (2.1) we have

$$\sigma_{zz}=\tfrac{3}{2}\sigma_0\int_0^{\pi}\frac{\cos^2\theta\sin\theta d\theta}{1+i(qV_F\sin\nu\cos\theta-\omega)\tau}. \qquad (3.1)$$

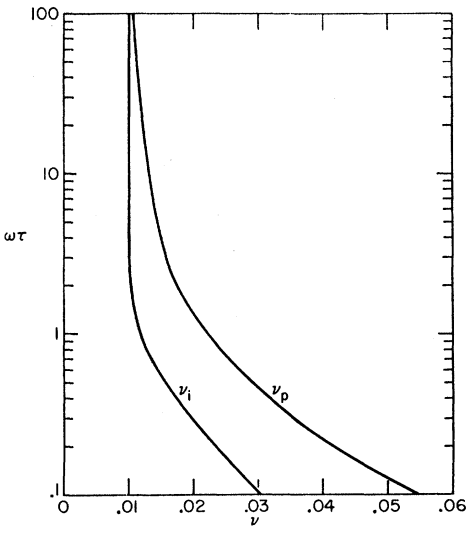

FIG. 2. The position of the peak and the inflection point in $(S_{11}-1)/[(m/m^*)(V_D/mV_F^2)^2]$ as a function of $\omega\tau$.

When $\sin\nu\sim V_S/V_F$ this term leads to a resonant absorption of energy. This resonance effect corresponds essentially to Reneker's qualitative arguments.

The peak in the attenuation occurs after we have passed ν_c, since at that angle only the carriers with the maximum drift velocity V_F experience acceleration. As we increase the angle of tilt past ν_c, carriers with less than the maximum drift velocity begin to contribute to the attenuation. Since there are more carriers contributing as we increase ν beyond ν_c, we have a corresponding increase in the attenuation. We can see this in Eq. (3.1). The integral is over the Fermi surface. The resonance occurs when $\cos\theta=V_S/V_F\sin\nu$, i.e., when the carriers located in a ring on the Fermi surface defined by the angle θ begin to contribute to the attenuation. When $\sin\nu<V_S/V_F$, the relation cannot be satisfied and there is no resonant absorption of energy. When $\sin\nu=V_S/V_F$ the carriers at the tip of

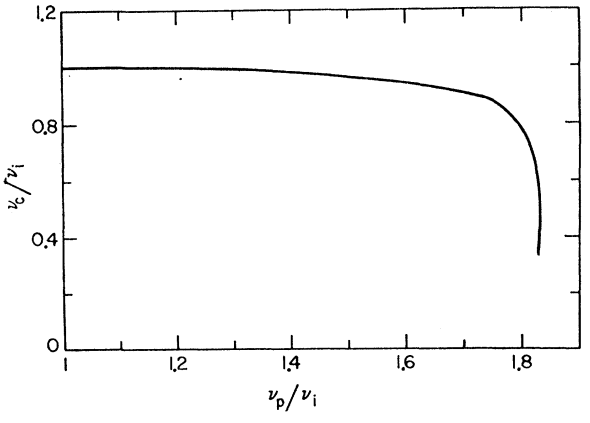

FIG. 3. The correction factor for $\omega\tau<1$. The ordinate is the ratio of the critical angle ν_c to the angle at which the point of inflection occurs ν_i. The abscissa is the ratio of the angle at which the peak occurs ν_P to the angle ν_i.

the Fermi surface ($\cos\theta=1$) begin to make a contribution to the attenuation and we have the onset of resonance. For $\sin\nu>V_S/V_F$ carriers from other segments of the Fermi surface start to contribute to the attenuation. Since the density of states is proportional to $\sin\theta$, the number of carriers contributing increases as we go beyond the critical angle. However, the drift velocity in the direction of the magnetic field is proportional to $\cos\theta$ and since it appears to the second power in the σ_{zz} component of the conductivity we have an additional factor of $\cos^2\theta$ in our integrand. The $\cos^2\theta$ factor causes the attenuation to decrease again despite the increasing density of states since $\cos\theta$ decreases as $1/\sin\nu$, i.e., the increase in the density of states is counterbalanced by the decrease in the component of the drift velocity along the magnetic field. The combined effect of the two factors is first to cause the attenuation to increase as we pass ν_c and then to cause it to decrease roughly as $1/\sin\nu$ as ν increases to $\pi/2$. This behavior results in a peak lying just beyond ν_c. The critical angle marks the onset of the increase and therefore it is reasonable to associate it with the point of maximum change in the attenuation rather than with the peak.

The broadening and decrease of the peak when $\omega\tau<1$ is the result of collisions which tend to destroy the phase relation between the sound wave and the carriers. This decreases the period of steady acceleration of the carriers and therefore also the attenuation. If a continuous wave technique is used to measure the derivative of the attenuation with angle then for $\omega\tau>1$, the critical angle ν_c and therefore the Fermi velocity can be determined exactly from the position of the peak in $d\alpha/d\nu$.

From the behavior of the attenuation with angle of tilt, it is not only possible to find the Fermi velocity but also to get a general check on the value of $\omega\tau$. One can estimate the value of $\omega\tau$ for our material for values of $\omega\tau$ between 0.1 and 100 from the graphs of $\omega\tau$ versus the position of the peak and the inflection point in Fig. 2.

IV. GENERAL FERMI SURFACES

While examining the attenuation of sound waves in a semimetal we have found a method for determining the Fermi velocity when we have a spherical Fermi surface. We examine in this section whether we can use the same method for determining V_F for a general Fermi surface. In the case previously treated, the resonance in the attenuation arose from the σ_{zz} component of the conductivity tensor where the z direction is the direction of the magnetic field. Extending the treatment of Chambers[4] to a space- and time-dependent electric field varying as $\exp i(\mathbf{q}\cdot\mathbf{r}-\omega\tau)$, we get for the ijth component of the conductivity tensor

$$\sigma_{ij}=\frac{e^2}{4\pi^3\hbar^2}\int_0^\infty\frac{\partial f_0}{\partial E}dE\int_{-\infty}^{\infty}dK_z\sum_\alpha m_\alpha\omega_\alpha\int_0^{2\pi/\omega_\alpha}dS\,V_i(S)\times\int_{-\infty}^{S}dS'V_j(S')\exp\left(i\omega-\frac{1}{\tau_\alpha}\right)(S-S')\times\exp-i\mathbf{q}\cdot\int_{S'}^{S}\mathbf{V}(S'')dS'',\quad(4.1)$$

where m_α and ω_α are the effective mass and the cyclotron frequency on the orbit α and the summation is over all orbits. We have assumed that the relaxation time is constant on an orbit. Since the velocity is periodic in S we can expand $\mathbf{V}$ in a Fourier series in S,

$$\mathbf{V}(S)=\sum_{n=-\infty}^{+\infty}\mathbf{V}(n)\exp(in\omega_\alpha S),\qquad\mathbf{V}^*(n)=\mathbf{V}(-n).\quad(4.2)$$

For closed orbits $V_x(0)=V_y(0)=0$, $V_z(0)\neq0$. Evaluating the expression Eq. (4.1) for the high-field case, i.e., $\omega_\alpha\gg10\mathbf{q}\cdot\mathbf{V}$, we obtain for the components of the conductivity tensor to the lowest order in $1/\omega_\alpha$

$$\sigma_{ij}=\frac{e^2}{2\pi^2\hbar^2}\int_0^\infty\frac{\partial f_0}{\partial E}dE\int_{-\infty}^{\infty}dK_z\sum_\alpha m_\alpha\tau_\alpha\sum_{n=-\infty}^{+\infty}\left[\frac{V_i(n)V_j^*(n)}{1+i[q_zV_z(0)-n\omega_\alpha-\omega]\tau_\alpha}-\frac{i\tau_\alpha}{\omega_\alpha}\times\frac{[q_zV_z(0)-n\omega_\alpha-\omega]}{1+i[q_zV_z(0)-n\omega_\alpha-\omega]\tau_\alpha}\mathbf{q}\cdot\sum_{m=1}^{\infty}\frac{1}{m}\{\mathbf{V}(m)V_i(n)V_j^*(n+m)+\mathbf{V}^*(m)V_i(n)V_j^*(n-m)\}\right].\quad(4.3)$$

Examining the term σ_{zz} which caused the resonance in the case of the spherical Fermi surface, we have to lowest order in $1/\omega_\alpha$

$$\sigma_{zz}=\frac{e^2}{2\pi^2\hbar^2}\int_0^\infty\frac{\partial f_0}{\partial E}dE\times\int_{-\infty}^{\infty}dK_z\sum_\alpha\frac{\tau_\alpha m_\alpha V_z^2(0)}{1+i[q_zV_z(0)-\omega]\tau_\alpha}.\quad(4.4)$$

Therefore we again have a resonance denominator in the σ_{zz} component of the conductivity. Because of the conditions of closed orbits [i.e., $V_x(0)=0$] and the high-field limit there are no resonance denominators for the σ_{xx} component.

In the case of open orbits, i.e., $V_x(0)\neq0$, we have instead of (4.4)

[4] R. G. Chambers, Proc. Roy. Soc. (London) **A238**, 344 (1956).

$$\sigma_{ii}=\frac{e^2}{2\pi^2\hbar^2}\int_0^\infty \frac{\partial f_0}{\partial E}dE \times\int_{-\infty}^{\infty}dK_z\sum_\alpha \frac{\tau_\alpha m_\alpha V_i^2(0)}{1+i[\mathbf{q}\cdot\mathbf{V}(0)-\omega]\tau_\alpha}, \quad (4.5)$$

for the σ_{xx} and σ_{zz} components of the conductivity. Therefore, we have resonance denominators for both of the components of the conductivity that contribute to the attenuation of the longitudinally polarized sound waves. Equation (4.5) indicates that for open orbits we have a drift along a direction perpendicular to the magnetic field as well as along the magnetic field. Therefore, the condition for the high-field tilt effect to take place is different for open orbits. The magnetic field must be tilted at an angle to the direction of propagation so that $\pi/2-\nu_c$ is the angle between the direction of propagation and the direction of the drift of carriers. Therefore, it is no longer the angle of tilt of the magnetic field that gives us ν_c.

For a closed Fermi surface, the following expressions have been derived for the drift velocity along the magnetic field and the effective mass in terms of the cross sectional area of the Fermi surface enclosed by the orbits[5,6]:

$$V_z(0)=\frac{-\hbar}{2\pi m_\alpha}\frac{\partial A}{\partial K_z}\Big)_E \qquad m_\alpha=\frac{\hbar^2}{2\pi}\frac{\partial A}{\partial E}\Big)_{K_z}. \quad (4.6)$$

[5] R. G. Chambers, Can. J. Phys. **34**, 1395 (1956).
[6] W. A. Harrison, Phys. Rev. **118**, 1190 (1960).

From Eq. (4.4) we see that we have a resonance denominator whenever the drift velocity along the field is a maximum. To plot out the Fermi velocity point by point on the Fermi surface, we want the maximum value of $V_z(0)$ to be associated with an extremum of the Fermi surface along the magnetic field where $V_z(0)=V_F$ as in the case of the spherical Fermi surface. However, from Eq. (4.6) we see that $V_z(0)$ does not have to be a local maximum at an extremum of the Fermi surface in general because of the behavior of m_α. Also there may be more than one maximum of $V_z(0)$ even for a singly connected piece of the Fermi surface. Therefore for a general Fermi surface the tilt effect is very complicated to interpret to say nothing about the complexities introduced by open orbits. However, for the tilt effect to occur at an observably large angle, V_F must be small and the Fermi surface must be close to a maximum or minimum in energy. Therefore the energy surfaces will often be ellipsoidal or nearly ellipsoidal so that analytical forms for the surface will usually be available and the appearance of open orbits will be unlikely.

We conclude, therefore, that whenever the tilt effect is observable, it permits a point-by-point plot of the velocity on the Fermi surface.

ACKNOWLEDGMENT

The author wishes to acknowledge the help and encouragement of Professor M. H. Cohen for suggesting this problem and for many valuable discussions.